ELSEVIER

Physica E 2 (1998) 325–329

PHYSICA E

Spontaneous lateral composition modulation in InAlAs and InGaAs short-period superlattices

D.M. Follstaedt[a,*], R.D. Twesten[a], J. Mirecki Millunchick[a], S.R. Lee[a], E.D. Jones[a], S.P. Ahrenkiel[b], Y. Zhang[b], A. Mascarenhas[b]

[a] *Sandia National Laboratories, Mail Stop 1056, Albuquerque, NM 87185-1056, USA*
[b] *National Renewable Energy Laboratory, Golden, CO 80401, USA*

Abstract

The microstructure of spontaneous lateral composition modulation along the [1 1 0] direction has been studied in $(InAs)_n/(AlAs)_m$ short-period superlattices grown by molecular beam epitaxy on (0 0 1) InP. X-ray diffraction and transmission electron microscopy show that global strain (ε) in the superlattice reduces the degree of composition modulation, which disappears for $|\varepsilon| > 0.7\%$. For tensile strains of $\varepsilon \approx +0.4\%$, we find that In-rich columns become regularly spaced and correlated with cusps in the growth surface. A similar correlation is seen in $(InAs)_n/(GaAs)_m$ short-period superlattices between the enriched columns and the peaks and valleys of $\{1\,1\,4\}_A$ facets on the surface. The enriched columns in the $(InAs)_n/(GaAs)_m$ layer (and the facets) extend for much longer distances ($\sim$ 0.2–0.4 μm) in the $[1\,\bar{1}\,0]$ direction than do the columns in the $(InAs)_n/(AlAs)_m$ layer ($\sim$56 nm).

Keywords: Lateral composition modulation; InAlAs; InGaAs; Strain; Short-period superlattice

Spontaneous composition modulation (CM) has been seen in many ternary III–V alloys [1], and in some materials, CM forms as a lateral modulation along a direction perpendicular to the epitaxial growth direction. Such modulation can produce important modifications of the opto-electronic properties, such as polarized optical emission, and is of interest for producing quantum-wire lasers and photodetectors. One method to induce and manipulate modulation is the growth of a short-period superlattice (SPS) by molecular beam epitaxy (MBE). This approach has been used by Cheng and co-workers [2–4] to produce lateral CM with $(InAs)_n/(GaAs)_m$ on InP and $(InP)_n/(GaP)_m$ on GaAs. We have grown $(InAs)_n/(AlAs)_m$ SPS on InP [5,6] and here discuss the role of global strain of the SPS layer on CM. X-ray diffraction (XRD) detects CM as lateral satellites lying along [1 1 0] on either side of the primary zincblende reflections [6]. The CM satellite intensity is strongest near zero strain, while relatively high strains of $|\varepsilon| > 0.7\%$ (either in tension or compression) cause the satellites to disappear. Selected specimens were examined with cross-section or plan-view transmission electron microscopy (TEM), and the observed

* Corresponding author. Tel.: + 1 505 844 2102; fax: + 1 505 844 2102; e-mail: dmfolls@sandia.gov.

1386-9477/98/$19.00
PII: S1386-9477(98)00068-X

degree of lateral CM correlates well with the CM satellite intensity. Moreover, for small tensile strain, $\varepsilon \approx +0.4\%$, the vertical layers are very regularly spaced and aligned with cusps in the growth surface, which we interpret as a synergistic coupling of In-rich layers with a locally enlarged lattice constant in the cusp. We also show that a similar alignment occurs in $(InAs)_n/(GaAs)_m$ on InP.

The $(InAs)_n/(AlAs)_m$ SPS was grown on (0 0 1) InP at 530°C under As-rich conditions. A buffer layer of approximately lattice-matched, random alloy InAlAs was first deposited using MBE. The buffer was grown at 0.7 ML/s, while the individual SPS layers were grown at approximately one-half this rate. The layers considered here have a total SPS period of $n + m \approx 3$–4 ML. The MBE growth rate was calibrated in situ using reflection high-energy electron diffraction oscillations. Cross-section and plan-view TEM specimens were prepared by mechanical polishing and Ar ion milling for examination with 200 or 300 keV electrons.

The composition and strain of the buffer and SPS were determined with lattice spacings from X-ray diffraction maps of reciprocal space around the (0 0 2) reflection. To do so, we note that the narrow width of the SPS reflections indicates essentially complete coherence, and selected examinations of (2 2 4) reflections with a component in the growth plane show full coherence; moreover, plan-view TEM images have not shown a misfit dislocation array. Taking the average in-plane lattice constant of the SPS ($a_{\parallel}$) to be equal to the substrate lattice constant (a_0) and measuring the average perpendicular lattice constant ($a_{\perp}$), we then assume that the composite elastic properties of the SPS are those of a random alloy with a tetragonal distortion and calculate the average lattice constant of the SPS (a_{epi}). We use a linear interpolation of lattice constant for the InAs–AlAs alloy system to obtain the average composition, and finally calculate the global strain of the layer with $\varepsilon = (a_{\parallel} - a_{epi})/a_{epi}$.

Fig. 1a shows integrated XRD intensities of the CM satellites as a function of average strain, while Fig. 1b is an example of an X-ray map showing half of the reciprocal space around the (0 0 2) zinc-blende reflection of the substrate and also showing the (0 0 2) reflection from the SPS and the CM satellite. The intensity shows a broad maximum near $\varepsilon \approx 0$ and decreases to zero at $\varepsilon \approx +0.7\%$

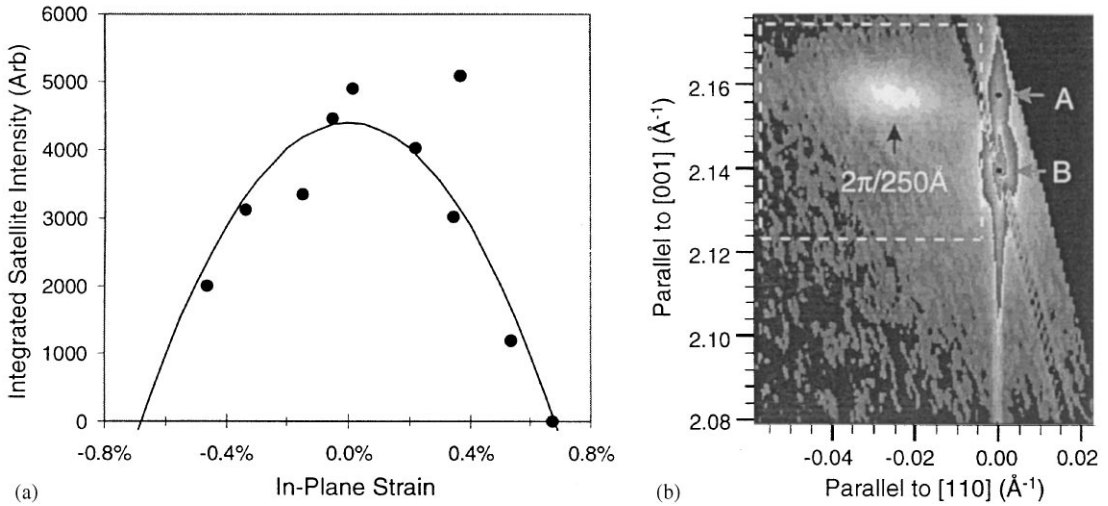

Fig. 1. (a) Plot of integrated XRD intensity of CM satellites versus in-plane strain of the $(InAs)_n/(AlAs)_m$ layers. The curve is a visual guide to indicate the deduced trend. (b) Reciprocal space intensity map around the (0 0 2) reflection for a specimen (#EA0122) of composition $In_{0.466}Al_{0.534}As$ and strain $\varepsilon = 0.37\%$. A and B indicate the positions of the (0 0 2) reflections for the SPS layer and the substrate, respectively, and the center of the CM satellite is indicated. The outlined rectangle shows the integration area for satellite intensity measurements.

(tension). Intensity also decreases for $\varepsilon < 0$ (compression), suggesting that it disappears near $\varepsilon \sim -0.7\%$. Cross-section TEM images for selected strains are shown in Fig. 2, using (0 0 2) dark-field conditions to maximize sensitivity of the contrast to composition variations [6]. The specimen in Fig. 2a has almost no strain ($\varepsilon \approx +0.05\%$) and shows intense, near-vertical columns going from the buffer across the SPS, with some wavering. The light areas are In-rich columns, and the horizontal SPS layers often show a dip on crossing them, as discussed further below. Our detailed analysis of the contrast in a similar specimen indicates that the Group III composition varies by tens of atomic percent [6]. Recent analysis using energy-dispersive X-ray spectroscopy with a sub-nanometer electron beam to obtain average local compositions shows that In is enriched to $In_{0.75}Al_{0.25}As$ in the narrow illuminated columns while between them Al is enriched to $In_{0.40}Al_{0.60}As$ [7].

Images of specimens with lower CM-satellite intensity are consistent with weaker modulation. The image in Fig. 2b from a specimen with $\varepsilon \approx -0.47\%$ shows less contrast, and it is difficult to trace some In-rich columns from bottom to top. Other images from such specimens show weak, wavy In-rich zones that sometimes appear to cross each other. The specimen with $\varepsilon \approx 0.67\%$ seen in Fig. 2c shows no evidence of CM with dark-field imaging, as predicted by the absence of a satellite in XRD. We conclude that as CM satellite intensity decreases, the columns seen in TEM show weaker contrast and become irregularly spaced and non-vertical, and that CM disappears for sufficiently large strain. We note that average modulation wavelengths, ranging from 15–30 nm as determined with the satellites, show no clear dependence on strain or CM intensity. There is an anti-correlation between the intensity of CM satellites and the SPS superlattice reflections, which are weaker for strong CM. This observation is consistent with the large composition variations, since the individual SPS layers in enriched zones must become more uniform with less vertical composition variation. In addition, the tilting of the SPS layers as they go through cusped regions reduces their spatial coherence and correspondingly, the intensity of the superlattice reflections.

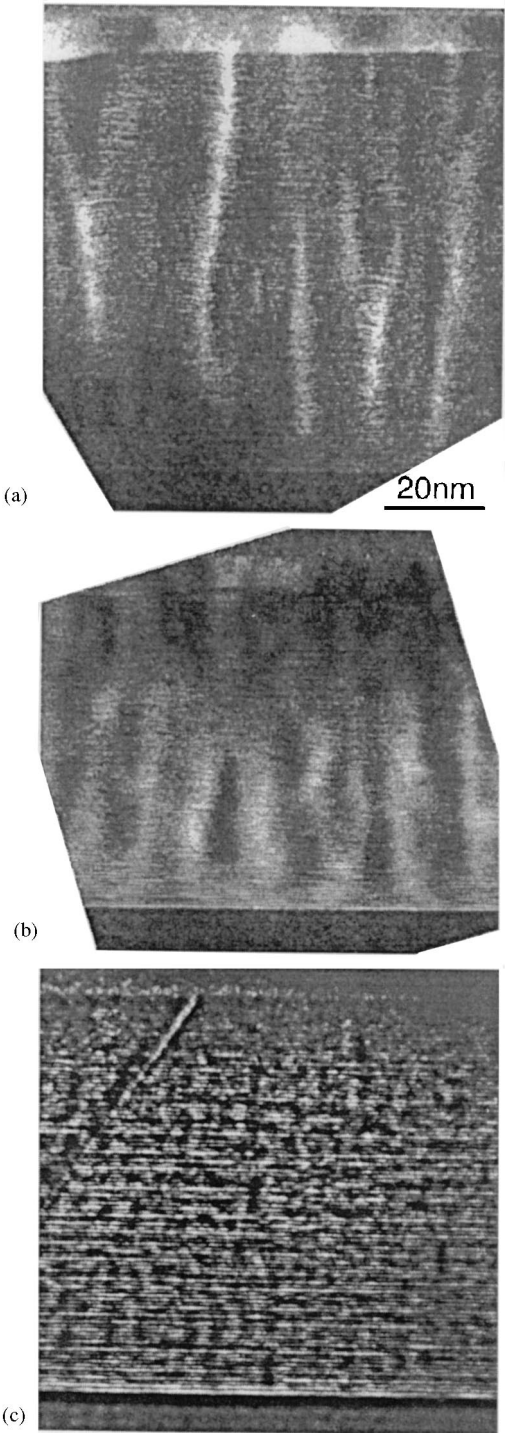

Fig. 2. Cross-section TEM images of $(InAs)_n/(AlAs)_m$ SPS layers for selected values of strain: (a) + 0.05% (specimen #EA0184), (b) − 0.47% (#EA0151), and (c) + 0.67% (#EA0121).

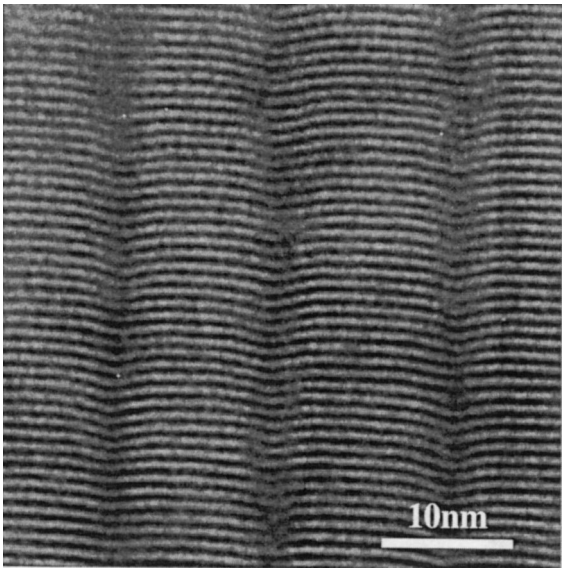

Fig. 3. Cross-section, bright-field TEM image of $(InAs)_n/(AlAs)_m$ SPS layers in tension ($\varepsilon \approx 0.43\%$). The SPS layers (black/white) show cusps located at dark In-rich CM columns (#511H).

For tensile strains $\varepsilon \approx 0.4$, the columns in TEM images still show strong contrast while the vertical layers are straight and regularly spaced, as seen in Fig. 3 (bright-field). Individual SPS layers can be followed horizontally across the structure and are seen to dip each time a dark In-rich layer is crossed. Since the individual layers are deposited serially, they reveal the history of the growth front and indicate that a cusp was continuously present at the position of each In-rich layer. When the growth surface of the strained layer is undulated, the material in the peaks is less constrained and can relax more than that in the valleys. In our material the lattice constant in the cusped regions remains expanded due to the overall tensile strain and is a better match to material enriched in larger In atoms. We infer that cusps on the growth surface become correlated with In-rich columns to reduce the overall strain energy of this tensile-strained material. The coupled surface cusps/CM layers apparently do not move laterally during growth, resulting in vertical, regularly spaced CM columns.

We have also grown $(InAs)_n/(GaAs)_m$ SPSs on (0 0 1) InP at 500°C, as seen for a tensile-strained

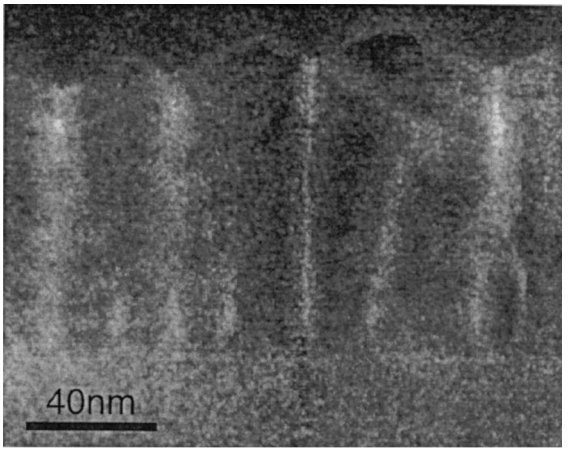

Fig. 4. Cross-section, (0 0 2) dark-field TEM image of $(InAs)_n/(GaAs)_m$ SPS layers in tension ($\varepsilon \approx 0.32\%$) having bright In-rich CM columns located under valleys on the surface (#EA0107).

layer ($\varepsilon \approx +0.32$) in Fig. 4 (dark-field). The bright In-rich columns are again nearly vertical and fairly regularly spaced at ≈ 32 nm apart, and end in the valleys of surface undulations. In this case, the surface has straight segments that correspond well to projections of $\{1\,1\,4\}_A$ surface facets tilted 19.5° from (0 0 1). The development of such growth facets was also seen by Okada et al. in tensile-strained InGaAs random alloys grown on InP [8]. For thick layers (~ 0.5 μm) they found In enrichment in columns directly below the valleys, with corresponding Ga enrichment at the peaks. In our $(InAs)_n/(GaAs)_m$ material, we find that CM begins very near the bottom of the SPS layer. While both our $(InAs)_n/(AlAs)_m$ and $(InAs)_n/(GaAs)_m$ SPSs show coupling of In-rich regions to valleys in tensile-strained layers, they differ dramatically in the extension of the CM columns in the orthogonal $[1\,\bar{1}\,0]$ direction. The enriched columns in $(InAs)_n/(AlAs)_m$ extend only about twice the [1 1 0] lateral period noted above, or about ~ 56 nm; however, those in $InAs_n/GaAs_m$ (and the facets) extend much farther, ~ 200–400 nm. The shorter extension along $[1\,\bar{1}\,0]$ in $(InAs)_n/(AlAs)_m$ may be due to the surface reconstruction changing from 2×4 (for In) to 2×1 (for Al) seen with RHEED during the SPS deposition [9]; the change in dimer row direction may inhibit growth along

[1 $\bar{1}$ 0]. No such change occurs between InAs and GaAs.

We conclude that global strain plays an important role in determining the degree of lateral CM in SPS layers. The elimination of CM in $(InAs)_n/(AlAs)_m$ for $|\varepsilon| \gtrsim 0.7\%$ agrees with an assessment by Hsieh and Cheng [4] that CM disappears near $\sim 1\%$. However, a small tensile strain ($\varepsilon \approx 0.4\%$) couples valleys in the undulated growth surface to In-rich columns with Al enrichment between them, and produces regularly spaced, vertical CM columns. This work also demonstrates that XRD measurements of CM satellite intensities can also be used to determine the relative degree of CM between specimens in an alloy system, which is important for ready assessment of specimens because XRD is less time-intensive than cross-section TEM.

The authors thank M.P. Moran for his skillful help in preparing cross-section TEM specimens. This work was supported by Division of Materials Sciences, Office of Basic Energy Sciences of the United States Department of Energy under contract DE-AC04-94Al85000. Sandia is a multiprogram laboratory operated by Sandia Corporation, a Lockheed Martin Company, for the United States Department of Energy.

References

[1] A. Zunger, S. Mahajan, Handbook on Semiconductors 3 (1994) 1399.
[2] K.Y. Cheng, K.C. Hsieh, J.N. Baillargeon, Appl. Phys. Lett. 60 (1992) 2892.
[3] K.C. Hsieh, J.N. Baillargeon, K.Y. Cheng, Appl. Phys. Lett. 57 (1990) 2244.
[4] K.C. Hsieh, K.Y. Cheng, Mat. Res. Soc. Symp. Proc. 379 (1995) 145.
[5] J. Mirecki-Millunchick, R.D. Twesten, S.R. Lee, D.M. Follstaedt, E.D. Jones, S.P. Ahrenkiel, Y. Zhang, H.M. Cheong, A. Mascarenhas, Appl. Phys. Lett. 70 (1997) 1402.
[6] R.D. Twesten, J. Mirecki Millunchick, S.P. Ahrenkiel, Y. Zhang, S.R. Lee, D.M. Follstaedt, A. Mascarenhas, E.D. Jones, Mat. Res. Soc. Symp. Proc. 441 (1997) 187.
[7] R.D. Twesten, unpublished composition data.
[8] T. Okada, G.C. Weatherly, D.W. McComb, J. Appl. Phys. 81 (1997) 2185.
[9] J. Mirecki Millunchick, R. Twesten, S.R. Lee, D.M. Follstaedt, E.D. Jones, S.P. Ahrenkiel, Y. Zhang, H.M. Cheong, A. Mascarenhas, J. Electronic Materials 26 (1997) 1048.